

Characterization of Cortical Networks during Motor Tasks in Humans

Fabrizio De Vico Fallani^{a,*}, Laura Astolfi^{a,b}, Febo Cincotti^a, Donatella Mattia^a, Fabio Babiloni^b and Alfredo Colosimo^b

^a IRCCS “Fondazione Santa Lucia”, Rome, Italy

^b Department of Human Physiology and Pharmacology, University “Sapienza”, Rome, Italy

* Corresponding Author: e-mail fabrizio.devicofallani@uniroma1.it

Abstract

The present study proposes a theoretical graph approach in order to evaluate the functional connectivity patterns obtained from high-resolution EEG signals. In particular, we evaluated the dynamics of the cerebral networks during the preparation and the execution of the foot movement in healthy subjects. High-resolution EEG represents a novel technique that can estimate non-invasively the cortical activity from the standard scalp EEG measurements. Brain functional networks are obtained by the time-varying Partial Directed Coherence, which describes the time-frequency relationships between the signals of different cortical regions. The evaluation of the time-varying topology of the estimated networks is addressed by means of graph theory, which describes concisely the complexity of the interconnected cerebral system. Altogether, our findings reveal new insights about the time-frequency dynamics of the cortical networks involved throughout the performance of a simple foot movement.

Introduction

The extraction of salient characteristics from brain connectivity patterns is an open challenging topic, since often the estimated cerebral networks have a relative large size and complex structure. Recently, it was realized that the functional connectivity networks estimated from actual brain-imaging technologies (MEG, fMRI and EEG) can be analyzed by means of the graph theory (Eiguluz et al., 2005; Salvador et al., 2005; Bartolomei et al., 2006; Stam et al., 2006; De Vico Fallani et al., 2007). Since a graph is a mathematical representation of a network, which is essentially reduced to nodes and connections between them, the use of a theoretical graph approach seems relevant and useful as firstly demonstrated on a set of anatomical brain networks (Watts et Strogatz, 1998). In those studies, the authors have employed two characteristic measures, the average shortest path L and the clustering index C , to extract respectively the global and local properties of the network structure. They have found that anatomical brain networks exhibit many local connections (i.e. a high C) and few random long distance connections (i.e. a low L). These values identify a particular model that interpolate between a regular lattice and a random structure. Such a model has been designated as “small-world” network in analogy with the concept of the small-world phenomenon observed more than 30 years ago in social systems (Milgram, 1967). In a similar way, many types of functional brain networks have been analyzed according to this

mathematical approach. In particular, several studies based on different imaging techniques (fMRI, MEG and EEG) have found that the estimated functional networks showed small-world characteristics (Achard et al., 2006; Basset et al., 2006; Stam et al., 2007). In the functional brain connectivity context, these properties have been demonstrated to reflect an optimal architecture for the information processing and propagation among the involved cerebral structures (Lago-Fernandez et al., 2000). However, the performance of cognitive and motor tasks as well as the presence of neural diseases has been demonstrated to affect such a small-world topology, as revealed by the significant changes of L and C. The aim of this study is to characterize the functional dynamics of the cortical network in every time-point during the preparation and the execution of the foot movement. Indeed the cortical connectivity is expected to rapidly change according to the different stages during the preparation and the execution of the foot movement.

Materials and Methods

Five voluntary subjects participated to the study (age, 26-32 years; five males). For the EEG data acquisitions, the participants were comfortably seated on a reclining chair in an electrically shielded and dimly lit room. They were asked to perform a dorsal flexion of their right foot, whose preference was previously attested by simple questionnaires. The movement task was repeated every 8 seconds, in a self-paced manner and 200 single trials were recorded by using 200 Hz of sampling frequency. The ROIs considered for the left (_L) and right (_R) hemisphere are the primary motor areas of the foot (MF_L and MF_R), the proper supplementary motor areas (SM_L and SM_R) and the cingulate motor areas (CM_L and CM_R). The bilateral Brodmann areas 6 (6_L and 6_R), 7 (7_L and 7_R), 8 (8_L and 8_R), 9 (9_L and 9_R) and 40 (40_L and 40_R) were also considered. In order to inspect the brain dynamics during the preparation and the execution of the studied movement, a time segment of 2 seconds was analyzed, after having centered it on the onset detected by a tibial EMG.

Cortical Activity Estimation

High-resolution EEG technology has been developed to enhance the poor spatial information of the EEG activity on the scalp and it gives a measure of the electrical activity on the cortical surface. Principally, this technique involves the use of a larger number of scalp electrodes (64-256). In addition, high-resolution EEG uses realistic MRI-constructed subject head models and spatial de-convolution estimations which are commonly computed by solving a linear inverse problem based on boundary-element mathematics (Le et Gevins, 1993; Babiloni et al., 2000). In the present study, the cortical activity was estimated from EEG recordings by using a realistic head model, whose cortical surface consisted of about 5000 triangles disposed uniformly. Each triangle represents the electrical dipole of a particular neuronal population and the estimation of its current density was computed by solving the linear inverse problem according to techniques described in previous works (see Appendix A for more details). In this way, the electrical activity in different Regions Of Interest (ROIs) can be obtained by averaging the current density of the various dipoles within the considered cortical area.

Each triangle represents the electrical dipole of a particular neuronal population and the estimation of its current density was computed by solving the linear inverse problem according to techniques described in previous works. In this way, the electrical activity in different Regions Of Interest (ROIs) can be obtained by averaging the current density of the various dipoles within the considered cortical area.

Functional Connectivity Estimation

Among the linear and nonlinear methods used to estimate functional brain connectivity, frequency-based methods are particularly attractive for the analysis of EEG or MEG data, since the activity of neural populations is often best expressed in this domain. Many EEG and/or MEG frequency-based methods that have been proposed in recent years for assessment of the directional influence of one signal on another are based mainly on the Granger theory of causality. Granger theory mathematically defines what a “causal” relation between two signals is. According to this theory, an observed time series $x(n)$ is said to cause another series $y(n)$ if the knowledge of $x(n)$'s past significantly improves prediction of $y(n)$; this relation between time series is not necessarily reciprocal, i.e., $x(n)$ may cause $y(n)$ without $y(n)$ causing $x(n)$. This lack of reciprocity allows the evaluation of the direction of information flow between structures. The advantages of MVAR modeling of multichannel EEG signals in order to compute efficient connectivity estimates have recently been stressed. Kus et al. (2004) demonstrated the superiority of MVAR multichannel modeling with respect to the pair-wise autoregressive approach. A very popular estimator, the Partial Directed Coherence (PDC), based on MVAR coefficients transformed into the frequency domain was recently proposed, as a factorization of the Partial Coherence (Baccalà et Sameshima, 2001) – see Appendix B for more details. The PDC is of particular interest because of its ability to distinguish direct and indirect causality flows in the estimated connectivity pattern. If another “true” flow exists from region x_2 to region x_3 , the PDC estimator does not add an “erroneous” causality flow between the signal recorded from region x_1 to region x_3 . This property is particularly interesting in its application to brain signals, where the interpretation of a direct connection between two cortical regions is straightforward.

Adaptive MVAR Models

The standard estimation of these methods requires the stationarity of the signals; moreover, with the estimation of a unique MVAR model on an entire time interval, transient pathways of information transfer remains hidden. To overcome this limitation, different algorithms for the estimation of MVAR with time dependent coefficients were recently developed. Hesse et al. (2003) proposed an application to MVAR estimation of the extension of the recursive least squares (RLS) algorithm with a forgetting factor. In the present study, this estimation procedure allows for the simultaneous fit of one mean MVAR model to a set of single trials, each one representing a measurement of the same task.

Fig.1 summarizes the results obtained by means of the methods illustrated throughout the present paragraph.

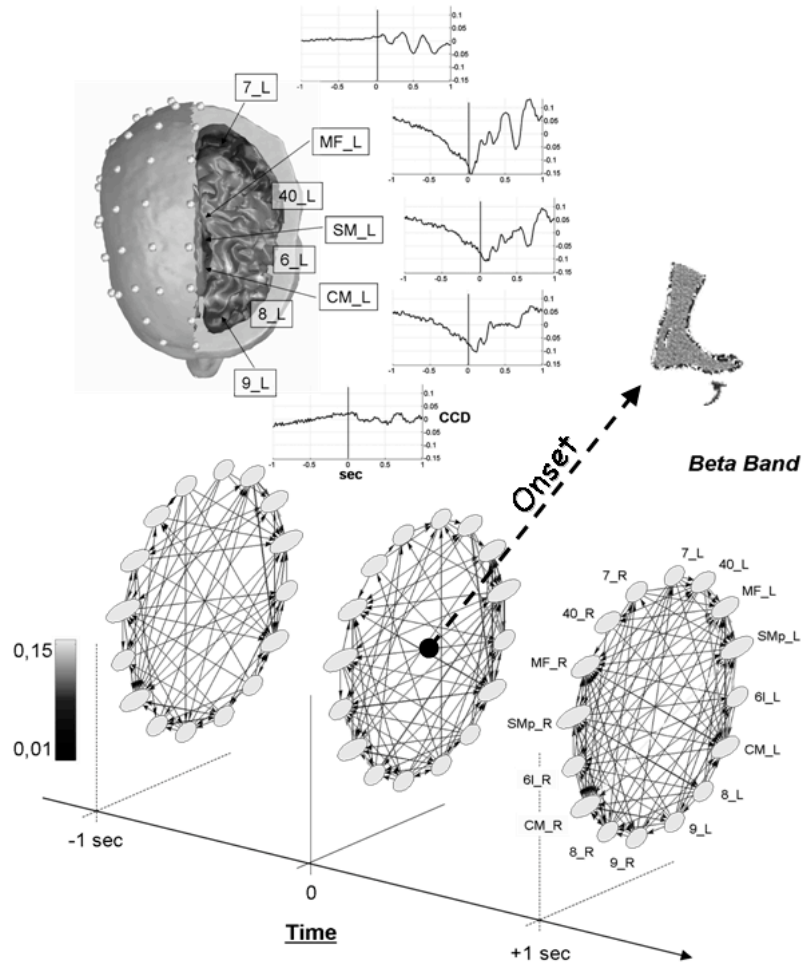


Fig. 1 - Up) Locations of the regions of interest (ROIs) on the left hemisphere of the cortex model together with their estimated temporal activity. Bottom) Time-varying cortical network in the Beta frequency band is shown for a representative subject. In particular, three instants are highlighted; one second before the onset, the onset itself and one second after the onset.

Graph Theory

A graph is an abstract representation of a network. It consists of a set of vertices (or nodes) and a set of edges (or connections) indicating the presence of some of interaction between the vertices. The adjacency matrix A contains the information about the connectivity structure of the graph. When a weighted and directed edge exists from the node i to j , the corresponding entry of the adjacency matrix is $A_{ij} \neq 0$; otherwise $A_{ij} = 0$.

Network Density

The simplest attribute for a graph is its density k , defined as the actual number of connections within the model divided by its maximal capacity; density ranges from 0 to 1, the sparser is a graph, the lower is its value. When dealing with weighted networks, a useful generalization of this quantity is represented by the weighted-density k_w , which evaluates the intensities of the links composing the network. In the present work, the link intensity encodes the level of Granger-causality between cortical time series. The mathematical formulation of the network density is given by the following:

$$k_w(A) = \sum_{i \neq j \in V} w_{ij} \quad (1)$$

Where A is the adjacency matrix and w_{ij} is the weight of the respective arc from the point j to the point i . $V=1 \dots N$ is the set of nodes within the graph.

Link Reciprocity

In a directed network, the analysis of *link reciprocity* reflects the tendency of vertex pairs to form mutual connections between each other. Here we computed the correlation coefficient index ρ (Garlaschelli and Loffredo, 2004), which measures whether double links (with opposite directions) occur between vertex pairs more or less often than expected by chance. The correlation coefficient can be written as follows:

$$\rho(A) = \frac{r(A) - k_w(A)}{1 - k_w(A)} \quad (2)$$

In this formula, r is the ratio between the number of links pointing in both directions and the total number of links, while k_w is the connection density that equals the average probability of finding a reciprocal link between two connected vertices in a random network. As a measure of reciprocity, ρ is an absolute quantity that directly allows one to distinguish between reciprocal ($\rho > 0$) and anti-reciprocal ($\rho < 0$) networks, with mutual links occurring more and less often than random, respectively. The neutral or areciprocal case corresponds to $\rho = 0$. Note that if all links occur in reciprocal pairs one has $\rho = 1$, as expected.

Motifs

By motif it is usually meant a small connected graph of M vertices and a set of edges forming a subgraph of a larger network with $N > M$ nodes. For each N , there are a limited number of distinct motifs. For $N = 3, 4$, and 5 , the corresponding numbers of directed motifs is 13, 199, and 9364 (Milo et al., 2002). The general formula showing the number of schemes compatible with a given number of nodes is not trivial. For the sake of simplicity this is not reported here. In this work, we focus on directed motifs with $N=3$. The 13 different 3-node directed motifs are shown in Fig. 2. Counting how many times a motif appears in a given network yields a frequency spectrum that contains important information on the network basic building blocks. Eventually, one can look at those motifs within the considered network that occur at a frequency significantly higher than in random graphs.

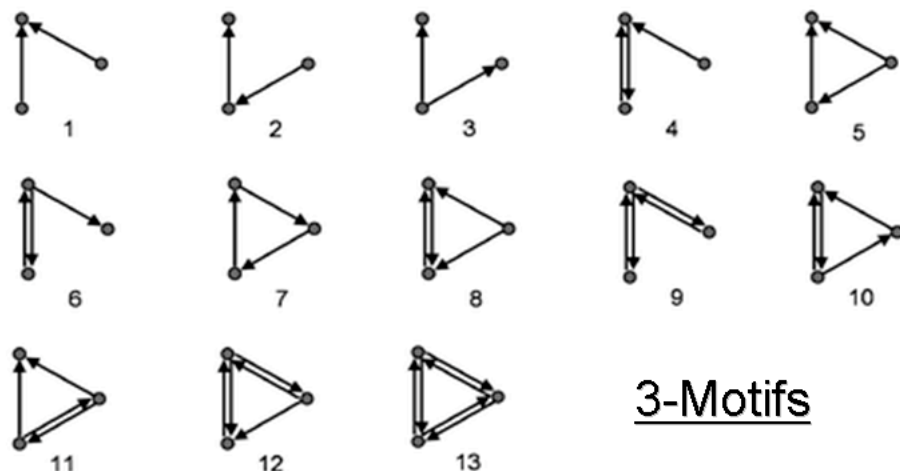


Fig. 2 – The 13 possible schemes of connectivity that can be achieved in a graph of 3 nodes. These connectivity patterns represent the possible building blocks constituting the estimated cortical networks.

Network Structure

Two measures are frequently used to characterize the local and global structure of unweighted graphs: the average shortest path L and the clustering index C . The former measures the efficiency of the passage of information among the nodes, the latter

indicates the tendency of the network to form highly connected clusters of vertices. Recently, a more general setup has been examined in order to investigate weighted networks. In particular, Latora and Marchiori (Latora et Marchiori, 2003) considered weighted networks and defined the efficiency coefficient e of the path between two vertices as the inverse of the shortest distance between the vertices (note that in weighted graphs the shortest path is not necessarily the path with the smallest number of edges). In the case where a path does not exist, the distance is infinite and $e = 0$. The average of all the pair-wise efficiencies e_{ij} is the global-efficiency E_g of the graph. Thus, global-efficiency can be defined as:

$$E_g(A) = \frac{1}{N(N-1)} \sum_{i \neq j \in V} \frac{1}{d_{i,j}} \quad (3)$$

where N is the number of vertices composing the graph. Since the efficiency e also applies to disconnected graphs, the local properties of the graph can be characterized by evaluating for every vertex i the efficiency coefficients of A_i , which is the sub-graph composed by the neighbors of the node i . The local-efficiency E_l is the average of all the sub-graphs global-efficiencies:

$$E_l(A) = \frac{1}{N} \sum_{i \in V} E_{glob}(A_i) \quad (4)$$

Since the node i does not belong to the sub-graph A_i , this measure reveals the level of fault-tolerance of the system, showing how the communication is efficient between the first neighbors of i when i is removed.

Results

The level of organization in the time-varying cortical networks during the foot movement was analyzed by computing the efficiency indexes E_g and E_l . The E_g and E_l indexes estimated in every subject from the respective cortical networks were contrasted with the ones obtained from the respective random structures. Fig. 3 shows the average Z-scores of the time-varying E_g (solid line) and E_l - (dotted line) of the connectivity patterns in the Beta frequency band.

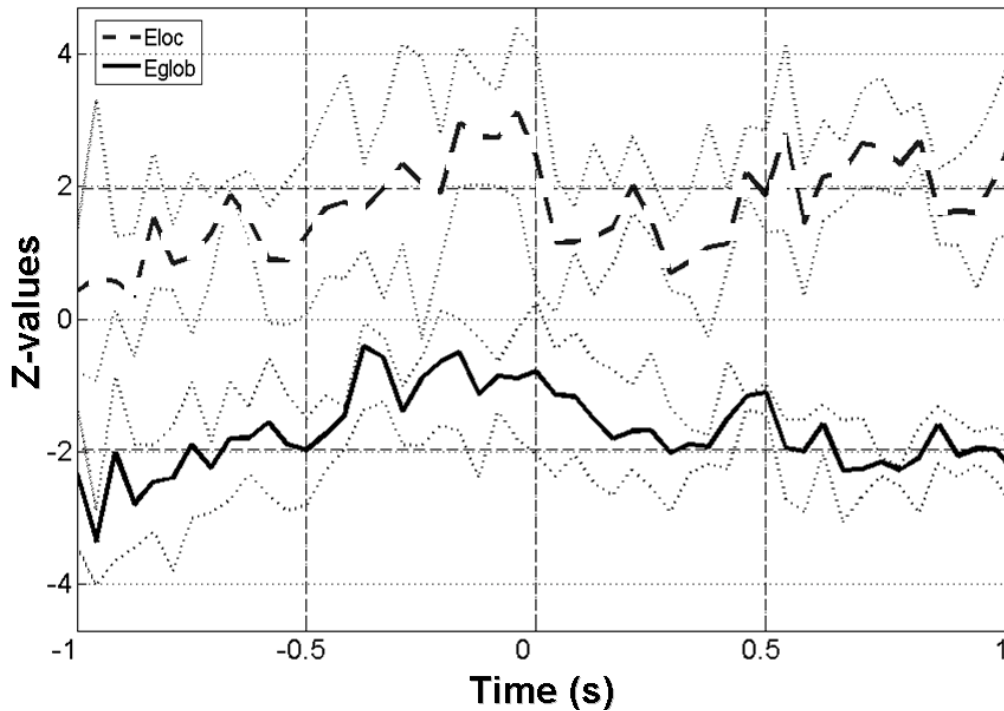


Fig. 3 – Average time-varying efficiency indexes. The lighter lines around the mean value indicate the time courses of the 25th and 75th percentile. The latency from the movement onset is shown on the x-axes.

In particular, one second before the onset (from about -1 to -0.5 s), the cortical networks mostly show low values of E_g and E_l , reflecting a weak pattern of communication characterized by long average distances and few clustering connections between the ROIs. Throughout the period closer to the execution of the movement (from about -0.5 s to the onset), both the global and local properties increase and in correspondence with it, we observe high values of E_g and E_l . This particular structure represents one of the best way in which the cortical areas communicate, since the relevant network presents simultaneously short links between each pair of ROIs and highly connected clusters (i.e. small-world architecture). After the onset (from the onset to +0.5 s), the estimated cortical networks show a typical random organization of the functional links, with a high E_g and a low E_l , reflecting the dense presence of wide-scope interactions among the ROIs, but a low tendency of the same cortical regions to form functional clusters. In the last period of the movement execution (from about +0.5 to +1 s) the estimated cortical networks mainly show high E_l values and low E_g values.

Fig. 4a) shows the average time-varying course of the weighted-density k_w in the Beta band during the analyzed period of interest. The average intensity of the network links during the preparation (from -0.5 s to the onset) is relatively low if compared with its maximum value reached in the following movement execution. In correspondence with this period the network structure presents the most efficient pattern of communication, as revealed by the estimated small-world characteristic.

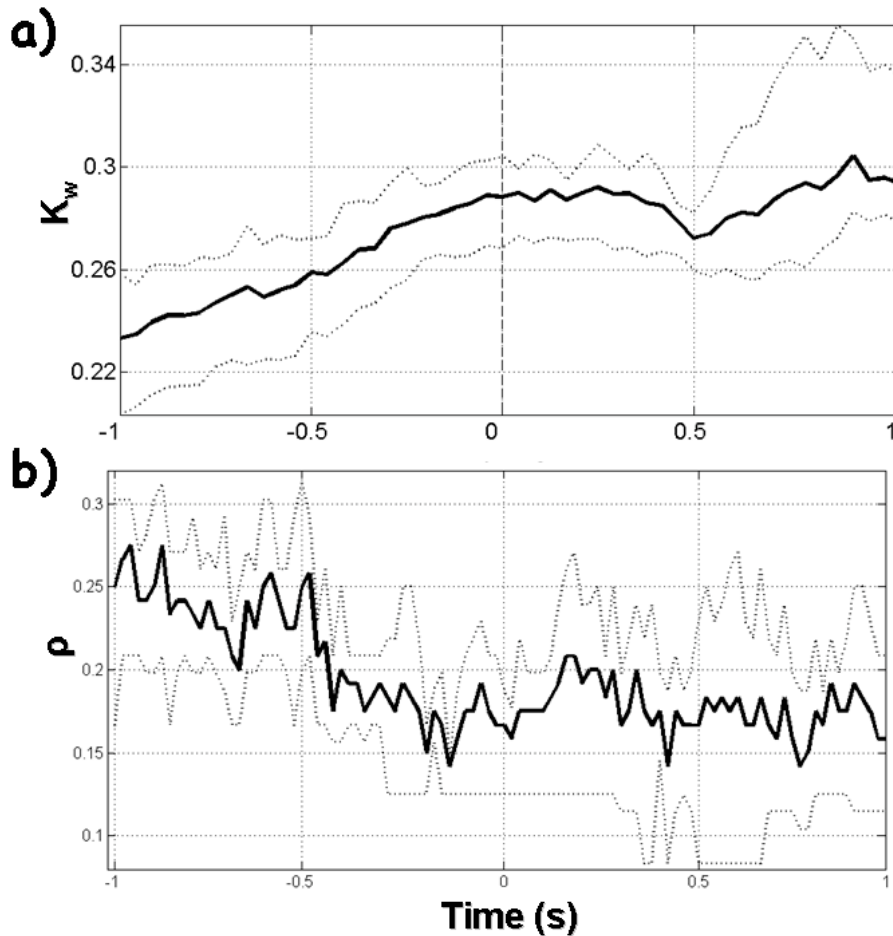


Fig. 4 – *a)* Average time-varying “weighted-density” in the Beta band. *b)* Average time-varying “reciprocity” during the period of interest in the Beta band. On y-axes the correlation coefficient ρ while time in seconds on x-axes.

The analysis of the average time-varying reciprocity index (Fig. 4b) revealed an interesting behavior during the preparation (from about -1 to -0.5 s) of the movement in the Beta frequency band. In such a period, the functional network moved from a high reciprocal state ($\rho \sim 0.25$) to a lower reciprocal state ($\rho \sim 0.17$) state. This aspect emphasizes the role of the early preparation in which a high level of mutual exchange of information is required to speed up the cortical process in expectation of the execution. Moreover, by tracking the evolving involvement of each single reciprocal connection (Fig. 5a) it is possible to observe their “persistence” during the entire period of interest. In particular, the persistent bilateral links between the cingulate motor areas and the supplementary motor areas (they correspond to the rows 58 and 69) in the Beta band reveals a novel aspect of such a connection that anyway was expected in a self-paced modality of movement generation, as in our experimental condition.

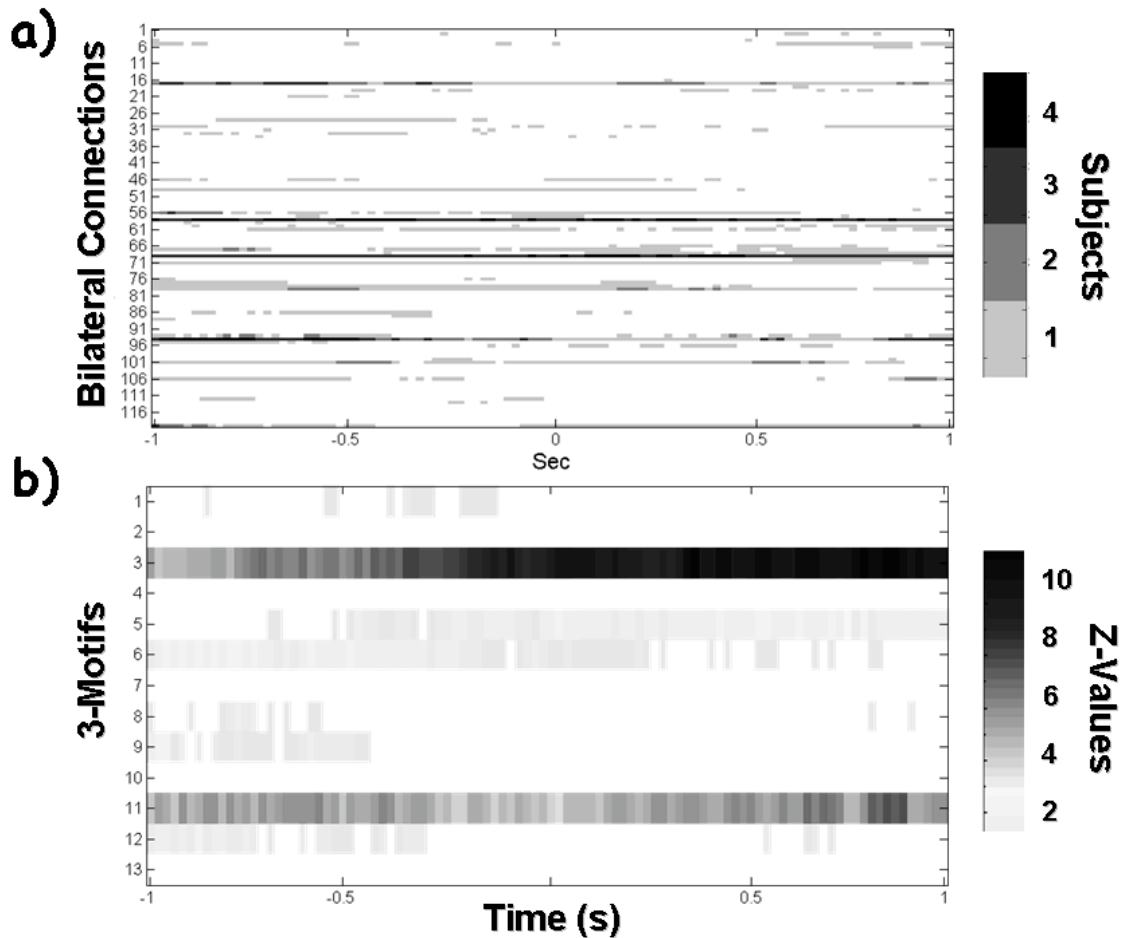


Fig. 5 – a) Time-varying persistence of the bilateral connections in the cortical network. On y-axes all the 120 possible reciprocal connections while time in seconds on x-axes. The colour of the line corresponding to a particular link codes the number of subjects that actually hold such a connection. b) Average time-varying 3-motif spectra. On y-axes all the 13 possible directed 3-motifs are listed while time in seconds is displayed on x-axes.

In Fig. 5b), we compared the 3-motif properties of real brain networks with random networks and we identified some motif classes that occurred more frequently during particular stages of the movement. Of particular interest is the significant ($p \ll 0.01$) “persistence” of the single-input motif (the third in the Fig. 2) that represented the highest recurrent pattern of interconnections during the entire evolution of the foot movement. The main function of this motif is known to involve the “activation” of several parallel pathways by a single activator (Shen-Orr et al., 2002).

Discussion

One of the interesting characteristics of the brain networks presented in this work is that such networks have no precise anatomical support, i.e. there is no particular cerebral structure that implements the network itself. Thus, those brain networks represent functional networks, which could change in topology and properties according to the specific subject’s behavior. Application of graph theory to small networks is rather new if compared to its usual employment in biological context. However, the need for the analysis of small cerebral networks has been recently underlined (Hilgetag et al. 2000; Micheloyannis et al. 2006; Stam et al. 2007). We would like to emphasize that the opportunity to deal with cortical activity permits the representation of the graph nodes as particular Brodmann areas on the cortex (Babiloni et al. 2005; De Vico Fallani et al.

2007). The use of raw EEG signals instead returns less powerful results, since the nodes within the network represent scalp electrodes, which could have indirect links with the cortical areas beneath them. In order to limit the discussion of the results, the present study has analyzed the cortical networks in the Beta (13-29 Hz) frequency band representing the spectral content principally involved in the preparation and the execution of simple motor acts (Pfurtscheller and Lopes da Silva, 1999). However, this methodology is not limited to a particular frequency band or a particular set of ROIs, since it can be adapted to investigate experimental tasks in any spectral content.

A possible use of the presented methodology could extract the significant features from the brain functional networks during the imagination of limb movements. The imagination of these motor acts would produce connectivity patterns that can be treated opportunely in the Brain Computer Interface context. The BCI is a recent field of research in which brain signals related to movement intention can be suitably treated to control external devices. According to this purpose the features extraction would improve as the brain functional relationships are supposed to reveal more information than simple cortical activity.

Footnotes

EEG – ElectroEncephaloGraphy
 MEG – MagnetoEncephaloGraphy
 MRI – Magnetic Resonance Imaging
 fMRI – functional Magnetic Resonance Imaging
 EMG – ElectroMioGraphy
 ROI – cortical Region Of Interest
 MVAR – MultiVariate AutoRegressive models
 PDC – Partial Directed Coherence

Supplementary Material

Appendix A

Head Models and Regions of Interest

In order to estimate cortical activity from conventional EEG scalp recordings, realistic head models reconstructed from T1-weighted MRIs are employed. Scalp, skull and dura mater compartments are segmented from MRIs and tessellated with about 5000 triangles. Then, the cortical regions of interest (ROIs) are drawn by a neuroradiologist on the computer-based cortical reconstruction of the individual head model by following a Brodmann's mapping criterion.

Estimation of Cortical Source Current Density

The solution of the following linear system:

$$Ax = b + n \quad (1.1)$$

provides an estimation of the dipole source configuration x which generates the measured EEG potential distribution b . The system includes also the measurement noise n , assumed to be normally distributed. A is the lead field matrix, where each j -th column describes the potential distribution generated on the scalp electrodes by the j -th unitary dipole. The current density solution vector ξ of Eq. 1.1 was obtained as:

$$\xi = \arg \min_x \left(\|Ax - b\|_M^2 + \lambda^2 \|x\|_N^2 \right) \quad (1.2)$$

where M , N are matrices associated to the metrics of data and source space, respectively; λ is a regularization parameter; $\| \dots \|_M$ represent the M-norm of the data space b and $\| \dots \|_N$ the N-norm of the solutions space x . The formula 1.2 represents a minimization problem also known as *linear inverse* problem.

As a metric of the data space the identity matrix is generally employed. However, the metric in the source space can be opportunely modified when hemodynamic information is available from recorded fMRI data. This aspect can notably improve the localization of the source activity. An estimate of the signed magnitude of the dipolar moment for each one of the 5000 cortical dipoles was then obtained for each time point. The instantaneous average of all the dipoles' magnitude within a particular ROI was used to estimate the average cortical activity in that ROI during the whole time interval of the experimental task

Appendix B

MultiVariate AutoRegressive Models

The approach based on multivariate autoregressive models (MVAR) can simultaneously model a whole set of signals. Let X be a set of estimated cortical time series:

$$X = [x_1(t), x_2(t), \dots, x_N(t)] \quad (2.1)$$

where t refers to time and N is the number of cortical areas considered. Given an MVAR process which is an adequate description of the data set X :

$$\sum_{k=0}^p \Lambda(k)X(t-k) = E(t) \quad (2.2)$$

where $X(t)$ is the data vector in time; $E(t) = [e_1(t), \dots, e_N(t)]$ is a vector of multivariate zero-mean uncorrelated white noise processes; $\Lambda(1), \Lambda(2), \dots, \Lambda(p)$ are the $N \times N$ matrices of model coefficients ($\Lambda(0) = I$); and p is the model order. The p order is chosen by means of the Akaike Information Criteria (AIC) for MVAR processes. In order to investigate the spectral properties of the examined process, the Eq. (2.2) is transformed into the frequency domain:

$$\Lambda(f)X(f) = E(f) \quad (2.3)$$

where:

$$\Lambda(f) = \sum_{k=0}^p \Lambda(k)e^{-j2\pi f \Delta t k} \quad (2.4)$$

and Δt is the temporal interval between two samples. Eq. (2.3) can then be rewritten as:

$$X(f) = \Lambda^{-1}(f)E(f) = H(f)E(f) \quad (2.5)$$

$H(f)$ is the transfer matrix of the system, whose element H_{ij} represents the connection between the j -th input and the i -th output of the system.

Partial Directed Coherence

In order to distinguish between direct and cascade flows, another estimator describing the direct causal relations between signals, the Partial Directed Coherence (PDC), was proposed in 2001. Like DTF, it is defined in terms of MVAR coefficients transformed to the frequency domain. The definition of Partial Directed Coherence (PDC) is:

$$\pi_{ij}(f) = \frac{\Lambda_{ij}(f)}{\sqrt{\sum_{k=1}^N \Lambda_{ki}(f) \Lambda_{kj}^*(f)}} \quad (2.9)$$

The PDC from j to i , $\pi_{ij}(f)$, describes the directional flow of information from the activity in the ROI $x_j(t)$ to the activity in $x_i(t)$, whereupon common effects produced by other ROIs $x_k(t)$ on the latter are subtracted leaving only a description that is exclusive from $x_j(t)$ to $x_i(t)$. PDC values are in the interval $[0 \ 1]$ and the normalization condition:

$$\sum_{n=1}^N |\pi_{ni}(f)|^2 = 1 \quad (2.10)$$

is verified. According to this condition, $\pi_{ij}(f)$ represents the fraction of the time evolution of ROI j directed to ROI i , as compared to all of j 's interactions with other ROIs. Figure 2 shows a schematic representation of the functional connectivity estimation from a set of high-resolution EEG signals to the cortical network.

References

- Achard S, Salvador R, Whitcher B, Suckling J and Bullmore Ed. 2006. A Resilient, Low-Frequency, Small-World Human Brain Functional Network with Highly Connected Association Cortical Hubs. *The Journal of The Journal of Neuroscience*, 26(1):63–72
- Babiloni F, Babiloni C, Locche L, Cincotti F, Rossini PM, Carducci F. 2000. High resolution EEG: source estimates of Laplacian-transformed somatosensory-evoked potentials using a realistic subject head model constructed from magnetic resonance images. *Med Biol Eng Comput*; 38:512-9
- Babiloni F, Cincotti F, Babiloni C, Carducci F, Basilisco A, Rossini PM, Mattia D, Astolfi L, Ding L, Ni Y, Cheng K, Christine K, Sweeney J, He B. 2005. Estimation of the cortical functional connectivity with the multimodal integration of high resolution EEG and fMRI data by Directed Transfer Function. *Neuroimage*; 24(1):118-3
- Baccalà L.A., Sameshima K, 2001. Partial Directed Coherence: a new concept in neural structure determination. *Biol Cybern*, 84: 463-474
- Bassett DS, Meyer-Linderberg A, Achard S, Duke Th, Bullmore E. 2006. Adaptive reconfiguration of fractal small-world human brain functional networks. *PNAS*, 103:19518-19523
- Bartolomei F, Bosma I, Klein M, Baayen JC, Reijneveld JC, Postma TJ, Heimans JJ, van Dijk BW, de Munck JC, de Jongh A, Cover KS, Stam CJ. 2006. Disturbed functional connectivity in brain tumour patients: evaluation by graph analysis of synchronization matrices. *Clin Neurophysiol*; 117:2039-2049
- De Vico Fallani F, Astolfi L, Cincotti F, Mattia D, Marciani MG, Salinari S, Kurths J, Gao S, Cichocki A, Colosimo A, Babiloni F. 2007. Cortical functional connectivity networks in normal and spinal cord injured patients: Evaluation by graph analysis. *Hum Brain Mapp*; 28:1334-6
- Eguiluz VM, Chialvo DR, Cecchi GA, Baliki M, Apkarian AV. 2005. Scale-free brain functional networks. *Phys Rev Lett*, 94:018102
- Garlaschelli D and Loffredo M I. 2004. Patterns of Link Reciprocity in Directed Networks *Phys Rev Lett* 93 268701
- Hesse W., Möller E., Arnold M., Schack B. 2003. The use of time-variant EEG Granger causality for inspecting directed interdependencies of neural assemblies. *Journal of Neuroscience Methods* 124: 27-44

- Hilgetag CC, Burns GAPC, O'Neill MA, Scannell JW, Young MP. 2000. Anatomical connectivity defines the organization of clusters of cortical areas in the macaque monkey and the cat. *Philos Trans R Soc Lond B Biol Sci*; 355:91-110
- Kus R, Kaminski M, Blinowska KJ . 2004. Determination of EEG activity propagation: pair-wise versus multichannel estimate. *IEEE Trans Biomed Eng.* Sep;51(9):1501-10
- Lago-Fernandez LF, Huerta R, Corbacho F, Siguenza JA. , 2000. Fast response and temporal coherent oscillations in small-world networks, *Phys. Rev. Lett.*; 84: 2758–61
- Latora V and Marchiori M. 2003. Economic small-world behaviour in weighted networks. *Eur Phys JB*; 32:249-263.
- Le J and Gevins A. , 1993. A method to reduce blur distortion from EEG's using a realistic head model. *IEEE Trans Biomed Eng* ; 40:517-28
- Micheloyannis S, Pachou E, Stam CJ, Vourkas M, Erimaki S, Tsirka V. 2006. Using graph theoretical analysis of multi channel EEG to evaluate the neural efficiency hypothesis. *Neuroscience Letters*; 402:273-277
- Milgram, S. 1967. [The Small World Problem](#), *Psychology Today*.; 60-67
- Milo R, Shen-Orr S, Itzkovitz S, Kashtan N, Chklovskii D and Alon U. 2002. Network motifs: simple building blocks of complex networks *Science* 298 824-7
- Pfurtscheller G, Lopes da Silva FH. 1999. Event-related EEG/EMG synchronizations and desynchronization: basic principles. *Clin Neurophysiol.* 110:1842–1857
- Salvador R, Suckling J, Coleman MR, Pickard JD, Menon D, Bullmore E. 2005. Neurophysiological Architecture of Functional Magnetic Resonance Images of Human Brain. *Cereb Cortex*; 15(9):1332-42
- Shen-Orr S, Milo R, Mangan S and Alon U. 2002. Network motifs in the transcriptional regulation network of *Escherichia coli* *Nature Genetics* 31 64-8
- Stam CJ, Jones BF, Manshanden I, van Cappellen van Walsum AM, Montez T, Verbunt JP, de Munck JC, van Dijk BW, Berendse HW, Scheltens P. 2006. Magnetoencephalographic evaluation of resting-state functional connectivity in Alzheimer's disease. *Neuroimage*; 32:1335-44
- Stam CJ, Jones BF, Nolte G, Breakspear M, Scheltens Ph. 2007. Small-world networks and functional connectivity in Alzheimer's disease. *Cereb Cortex*; 17:92-99
- Watts DJ and Strogatz SH. 1998. Collective dynamics of 'small-world' networks. *Nature*; 393:440-2